
A STUDY ON THE INTERSECTION OF GPU UTILIZATION AND CNN INFERENCE

Jack Kosaian^{1*} Amar Phanishayee²

ABSTRACT

There has been significant progress in developing neural network architectures that both achieve high predictive performance and that also achieve high application-level inference throughput (e.g., frames per second). Another metric of increasing importance is GPU utilization during inference: the measurement of how well a deployed neural network uses the computational capabilities of the GPU on which it runs. Achieving high GPU utilization is critical to increasing application-level throughput and ensuring a good return on investment for deploying GPUs.

This paper analyzes the GPU utilization of convolutional neural network (CNN) inference. We first survey the GPU utilization of CNNs to show that there is room to improve the GPU utilization of many of these CNNs. We then investigate the GPU utilization of networks within a neural architecture search (NAS) search space, and explore how using GPU utilization as a metric could potentially be used to accelerate NAS itself. Our study makes the case that there is room to improve the inference-time GPU utilization of CNNs and that knowledge of GPU utilization has the potential to benefit even applications that do not target utilization itself. We hope that the results of this study will spur future innovation in designing GPU-efficient neural networks.

1 INTRODUCTION

Convolutional neural networks (CNNs) have been widely used in many image- and video-processing tasks. In addition to designing CNNs that achieve high accuracy on a particular task, a large body of work has focused on designing CNNs that also operate with low latency or high application-level throughput (e.g., frames per second) (Redmon et al., 2016; Kang et al., 2017). The latency and throughput of CNNs has also been bolstered through advances in hardware, such as through GPUs that offer specialized compute units for accelerating neural networks (e.g., NVIDIA’s Tensor Cores) (NVIDIA, 2017; 2018; a).

An important, yet often overlooked, metric for CNN inference on GPUs is *GPU utilization*: the measure of the fraction of a GPU’s peak computational performance that CNN inference can sustain. Recent GPUs offer hundreds of TFLOPs/sec. of compute bandwidth. It is critical that these GPUs be highly utilized, with software running on an GPU ideally achieving TFLOPs/sec. near the GPU’s theoretical peak. Poorly utilizing a GPU leads to a poor return on investment for purchasing and deploying an accelerator, and leaves room on the table to further improve latency or throughput.

Despite the importance of GPU utilization in application performance and operational efficiency, GPU utilization is often overlooked in designing CNNs. While prior work has considered GPU utilization in highly specific settings (Kosaian et al., 2021), the GPU utilization of general-purpose CNNs has been less-widely studied. Other techniques aim to improve GPU utilization at the system level by efficiently co-executing multiple CNNs (Jain et al., 2018; Narayanan et al., 2018; Wang et al., 2021), but these works do not consider improving the GPU utilization of a single CNN, which remains important in many settings.

This paper aims to fill this void by performing a multi-faceted study of GPU utilization for CNN inference. We focus specifically on GPUs, as they are widely used in datacenter settings for performing high-throughput inference. We decompose our study into three parts:

First, we survey the GPU utilization of CNNs used for image classification. We consider both CNNs developed manually as well as those found by architecture search techniques, and also consider CNNs that vary in terms of accuracy and throughput. Our survey reveals a mixed landscape of GPU utilization: some CNNs are capable of achieving high GPU utilization, while others fall significantly short, even when using large batch sizes. Notably, many of the CNNs that poorly utilize GPUs are on the Pareto frontier of other important metrics, such as accuracy and throughput. This leads one to question whether the accuracy and/or throughput of these CNNs could be further bolstered by

*Work done as a Microsoft Research intern¹Carnegie Mellon University²Microsoft Research.

increasing GPU utilization.

Based on this survey, we next investigate techniques to improve the GPU utilization of CNNs that poorly utilize GPUs. Specifically, we focus on CNNs that have low arithmetic intensity—a property of a CNN that drives its GPU utilization, and which will be defined in detail in §2. We investigate the potential for techniques previously proposed for increasing the arithmetic intensity of small, specialized CNNs (Kosaian et al., 2021) to also provide benefit for general-purpose CNNs. We find that these techniques do indeed transfer to the domain of general-purpose CNNs in terms of improving arithmetic intensity, throughput, and GPU utilization, though we do not consider whether the resultant CNNs maintain high accuracy. This offers promising potential for improving the GPU utilization of general-purpose CNNs.

Finally, we consider the role of GPU utilization in neural architecture search (NAS). Alongside the analysis presented above, we additionally study the accuracy, throughput, and GPU utilization of CNNs a search space from NATS-Bench (Dong et al., 2021). Our study reveals a positive correlation between GPU utilization and accuracy within this search space. This correlation leads us to consider whether GPU utilization can be used as a metric in place of accuracy during NAS to speed up the overall search process. GPU utilization is a significantly cheaper metric to measure than accuracy during NAS; measuring GPU utilization requires only measuring throughput and analyzing the FLOPs performed by a CNN, whereas measuring accuracy requires training a candidate NN. Thus, if possible, using GPU utilization in place of accuracy in NAS could reduce the search time in NAS. We investigate this question further by considering the use of GPU utilization as an approximate filtering metric to reduce the number of candidates in NAS required for full accuracy evaluation. While our preliminary results do not yield improvements in NAS time or search quality, we conclude that future NAS techniques should consider how they can leverage GPU utilization to potentially improve the NAS search process.

Overall, this paper does not propose novel techniques with positive results. Rather, its aim is to survey GPU utilization in CNN inference and to consider how it could be improved or used in other aspects of the machine learning lifecycle. This survey indicates that there is room for improvement in GPU utilization within CNN inference. Improving GPU utilization offers promises not only for improved operational efficiency, but also for improving the throughput and/or accuracy of CNNs themselves. We hope that our findings will spur further research in improving and exploiting GPU utilization.

A note on the setting of this paper: The research performed in this paper took place in the summer of 2021, as

did the majority of the writing of this paper. We leveraged CNNs, GPUs, and software libraries that were widely used at the time, but they may either have been superseded or improved as of the release of this paper. Advancements in network design, hardware, and software may modify our findings.

2 BACKGROUND AND RELATED WORK

In this section, we define GPU utilization, why it is important, and how to achieve high GPU utilization. We additionally describe related work on increasing GPU utilization.

2.1 GPU utilization

Processors, whether CPUs, GPUs, or specialized accelerators, have a theoretical peak number of operations that they can perform per second. This metric is determined by the number of processing elements on the processor that can be used concurrently, the number of operations each processing element can perform per cycle, and the number of cycles the processor performs per second. This theoretical peak value is typically measured in terms of the number of floating-point operations that can be performed per second (i.e., FLOPs/sec.).

However, not all software running atop a processor is capable of achieving the theoretical peak FLOPs/sec. of the processor. This gives rise to the definition of utilization we leverage in this work: the fraction of a processor’s peak FLOPs/sec. that a computation can sustain. As this paper focuses on GPUs, we will refer to this utilization as “GPU utilization” for the remainder of this discussion.

Why is GPU utilization important? Maintaining high GPU utilization is important for multiple reasons. First, from the perspective of an application, underutilizing a GPU leaves application-level performance (e.g., frames per second) on the table; underutilization means that one could potentially get more application-level value from the GPU on which they are already running. Second, underutilization leads to poor operational efficiency. GPUs are expensive and power hungry. Thus, underutilizing a GPU leads to a poor return on infrastructure investment, as well as less sustainable infrastructure. Thus, it is important for software to highly utilize GPUs.

What is needed for a CNN to highly utilize a GPU? A prerequisite for achieving the peak FLOPs/sec. of a GPU is that the computation in question be compute bound: a compute-bound computation performs enough computation to keep all processing elements on a processor busy at all times.

To determine whether a computation is compute bound, we turn to a popular performance model (Williams et al., 2009).

Intuitively, a compute-bound computational kernel is one that spends more time performing computation than it does reading/writing memory:

Compute time > Memory load/store time

$$\frac{\text{FLOPs}}{\text{Compute Bandwidth}} > \frac{\text{Bytes}}{\text{Memory Bandwidth}}$$

Here, ‘‘FLOPs’’ is the number of arithmetic operations performed by the kernel, ‘‘Bytes’’ is the amount of data the kernel transfers to/from memory, ‘‘Compute Bandwidth’’ is the GPU’s peak FLOPs/sec., and ‘‘Memory Bandwidth’’ is the GPU’s memory bandwidth (bytes/sec). Rearranging this inequality to pair properties of the kernel on the left-hand side and properties of the GPU on the right-hand gives:

$$\frac{\text{FLOPs}}{\text{Bytes}} > \frac{\text{Compute Bandwidth}}{\text{Memory Bandwidth}} \quad (1)$$

The left-hand ratio of Equation 1 is the kernel’s arithmetic intensity: the ratio between the FLOPs the kernel performs and the bytes it transfers to/from memory. The right-hand ratio is the GPU’s compute-to-memory-bandwidth ratio (CMR).

The inequality in Equation 1 indicates that a computational kernel must have arithmetic intensity higher than the CMR of the GPU on which it executes in order to have the possibility of achieving the peak FLOPs/sec. of the GPU. It is important to note that satisfying the inequality in Equation 1 is only a prerequisite to achieving high utilization; doing so does not guarantee that one will achieve peak FLOPs/sec.. A kernel satisfying this inequality can still poorly utilize a processor if the implementation of the kernel does not make efficient use of resources on the processor (e.g., through not using vector instructions or inefficiently using the memory hierarchy).

2.2 Effects of model and input size on GPU utilization

We now describe the effects that batch size and CNN size have on GPU utilization.

In discussing each of these components, it is helpful to have a slightly deeper view of arithmetic intensity for CNNs. The arithmetic intensity of any layer of a CNN can be (abstractly) written as:

$$\frac{\text{FLOPs}}{\text{Input bytes} + \text{Weight bytes} + \text{Output bytes}} \quad (2)$$

‘‘FLOPs’’ is, again, the number of arithmetic operations performed by the layer. ‘‘Input bytes’’ is the total size of the layer’s input activations, ‘‘Output bytes’’ is the total size of output activations written by the layer to memory for processing by the next layer, and ‘‘Weight bytes’’ is the total size of the layer’s weights.

In defining the aggregate arithmetic intensity of a CNN as a whole, one sums the FLOPs performed across all layers, sums the bytes transferred to/from memory by all layers, and divides these components. This metric is not as useful as the arithmetic intensities of individual layers of a CNN, as CNN inference is performed on a per-layer basis. Nevertheless, it gives a broad notion of how compute- or memory-bandwidth-bound a CNN as a whole is likely to be. Finally, we note that our analysis here assumes that common optimizations that increase arithmetic intensity are performed, such as fusing non-linear layers to the preceding linear layers to minimize memory traffic.

Effect of batch size. The input to a CNN is a batch of N images each with resolution $H \times W$ and C channels (e.g., $C = 3$ for RGB images). Here, we will focus on the effect of batch size N on the arithmetic intensity of a CNN, as high-throughput vision applications often leverage large batch sizes.

A layer in a CNN operates (abstractly) by (1) loading the layer’s weights from memory, (2) loading the input activations to the layer from memory, (3) computing over the input activations using layer weights, and (4) writing the outputs of the layer to memory.

Each of steps 2, 3, and 4 above scale linearly with increasing batch size, while step 1 remains a constant cost regardless of the batch size used. Translating these scaling factors to Equation 2, we see that increasing batch size leads to a linear increase in the numerator and a sub-linear increase in the denominator (because ‘‘Weight bytes’’ does not increase with batch size). Thus increasing batch size increases arithmetic intensity. The increase in arithmetic intensity from increased batch size is intuitive: operating at a larger batch size better amortizes the cost of loading a layer’s weights from memory.

However, increasing batch size eventually leads to diminishing returns in arithmetic intensity: once batch size has been increased to the point in which loading layer weights accounts for negligible memory traffic, further increasing batch size provides an insignificant increase in arithmetic intensity. Prior work has illustrated this limit for CNNs developed through model specialization (Kosaian et al., 2021). For these CNNs, arithmetic intensity still remains lower than the CMR of server-grade GPUs even when operating at large batch sizes.

Effect of CNN size. Large CNNs, such as those with more channels per convolutional layer, typically perform more FLOPs than small CNNs. As a result, they typically have higher arithmetic intensity, and thus also typically better utilize GPUs. However, this increased FLOP count typically comes at the expense of lower application-level throughput

or higher latency.

On the other hand, decreasing the size of a CNN typically reduces the number of FLOPs it performs. This often leads to higher application-level throughput or lower latency, at the expense of lower arithmetic intensity, and thus lower GPU utilization. For example, techniques like model scaling (e.g., through EfficientNets (Tan & Le, 2019)) and model specialization produce CNNs that can operate with higher throughput than larger CNNs, but which typically poorly utilize GPUs (Kosaian et al., 2021).

2.3 Related work on high GPU utilization

We now highlight related work aimed at improving the GPU utilization of CNNs.

Improving utilization via multi tenancy. One approach to increase GPU utilization is to concurrently execute multiple neural networks on a single GPU at once. This technique has been explored both for training neural networks, such as through scheduling systems (Xiao et al., 2018; Gu et al., 2019), as well as for inference, by fusing and co-executing similar layers of distinct neural networks together (Narayanan et al., 2018; Jain et al., 2018; Wang et al., 2021) or through better management of GPU resources (Yu & Chowdhury, 2020).

In contrast to these works, our focus in this work is on analyzing the GPU utilization of performing inference over a single CNN, rather than a group of co-scheduled CNNs. Techniques used to improve the GPU utilization of a single CNN can be used alongside these co-scheduling techniques.

Designing hardware-efficient CNNs. An alternative line of work has focused on designing CNNs that efficiently make use of a given device. This has been leveraged to develop low-latency CNNs for mobile deployments (e.g., (Wu et al., 2019)), as well as architecture search techniques that can achieve high performance across a variety of hardware backends (Cai et al., 2019).

Along this same line of work, multiple works have considered developing GPU-efficient CNNs. These works either optimize for metrics that are proxies for GPU utilization (e.g., frames/sec. on a GPU) (Molchanov et al., 2021; Ridnik et al., 2021), or by optimizing for a metric closely related to GPU utilization, such as arithmetic intensity (Zhou et al., 2018). Other work has proposed transformations to CNNs in specific settings to improve their GPU utilization (Kosaian et al., 2021).

In contrast to these works, our focus in this paper is primarily in surveying the GPU utilization of CNN inference. In doing so, we evaluate some of the networks discovered by techniques listed above.

System support for GPU-efficient inference. There have been many recent works that aim to make better use of the underlying hardware on which neural network inference is executed (Chen et al., 2018; NVIDIA, c). However, as described above, achieving high GPU utilization requires not only that software be optimized, but also that a CNN have a high enough arithmetic intensity. Thus, in this work, we focus on the GPU utilization of CNN inference primarily by studying the arithmetic intensity of CNNs. However, we note that all of our results involve executing CNNs when using the GPU-optimized TensorRT SDK (NVIDIA, c).

3 ANALYZING GPU UTILIZATION IN CNN INFERENCE

We begin our study of GPU utilization in CNN inference by surveying the GPU utilization of a variety of CNNs. Through this study, we establish that these CNNs operate within a wide spectrum of GPU utilization. We conclude by discussing and evaluating a potential opportunity to improve GPU utilization.

As described in §1, the research performed in this paper took place in the summer of 2021. We leveraged CNNs, GPUs, and software libraries that were widely used at the time, but they may either have been superseded or improved as of the release of this paper; e.g., our CNNs do not reflect the recent trend of using transformers in vision tasks. Advancements in network design, hardware, and software may modify our findings.

3.1 Setup

We analyze the GPU utilization of CNNs by executing them atop a V100 GPU through the TensorRT SDK and when using FP16 datatypes, which involves the use of Tensor Cores (NVIDIA, b). We choose this setting because, at the time when this research was performed, the V100 was a widely-deployed GPU in datacenters today used for high-throughput applications. Our microbenchmarks reveal a maximum achievable performance of 100 TFLOPs/sec. on the device used for evaluation, which is on par with that reported in prior work (Jia et al., 2018). We execute each CNN at the maximum batch size that it can fit within the GPU’s memory. Operating at large batch size is common for high-throughput applications.

We analyze 103 CNNs used for image classification from the `timm` repository (Wightman, 2019), as well as those used for the V100 in the once-for-all network (Cai et al., 2019). The `timm` repository contains implementations of a large collection of CNNs, many of which have, at some point in time, achieved state-of-the-art accuracy on popular tasks, or state-of-the-art results on the Pareto frontier of accuracy and latency/FLOP count. CNNs within this repository include

both those that have been hand crafted as well as those that have been discovered through architecture search techniques. We only include CNNs that compiled with TensorRT at the time of our experimentation. We additionally measure the performance of CNNs specialized for the V100 from Once-For-All networks (Cai et al., 2019). A list of all CNNs considered is provided in §A.

Measuring GPU utilization. The metric of interest for GPU utilization is the fraction of the peak achievable FLOPs/sec. of the V100 GPU that a CNN can sustain. To measure the FLOPs/sec. achieved by the CNN, we measure the throughput of the CNN in terms of images/second over 10000 batches and multiply this by the FLOP count of the CNN when operating over a single image. This value is then divided by the GPU’s peak achievable FLOPs/sec. to obtain GPU utilization as a fraction. We find the V100 to achieve 100 TFLOPs/sec. in FP16 when utilizing Tensor Cores on a large matrix multiplication, and use this as the peak achievable FLOPs/sec. of the device. We use input and output sizes commonly used for ImageNet (Russakovsky et al., 2015): images are of resolution 224×224 , and each CNN produces a prediction vector over 1000 classes.

Reporting accuracy. We additionally report the accuracy of CNNs on the ImageNet dataset. We do not train these CNNs ourselves, but rather report the accuracies of these CNNs that have been attained within the `timm` and `once-for-all` network repositories.

3.2 Analysis of CNN GPU utilization

Figure 1 plots the accuracy, throughput, and GPU utilization of all CNNs considered. Plotting these CNNs along any two of these three metrics results in a two-dimensional Pareto frontier. Overall, we find that only one CNN, TRResNet-M, sits along all three Pareto frontiers. It is interesting to note that the TRResNet family of CNNs was designed specifically to operate efficiently on GPUs (Ridnik et al., 2021).

We next analyze each of the two-dimensional Pareto frontiers displayed in Figure 1.

Throughput-accuracy. Figure 1a plots each CNN according to its achieved throughput and accuracy. This is a popular frontier to consider, as throughput is an important application-level metric targeted by many systems. We observe a general trend that CNNs with higher throughput typically have lower accuracy. This is likely due to these high-throughput CNNs being smaller in size, both in terms of parameters and FLOP count. Reducing CNN size often brings improvements in throughput or latency at the expense of lower accuracy. We additionally observe a large cluster of CNNs that have lower throughput and higher accuracy. This is likely an artifact of sampling bias, as many of the

CNNs we considered were designed primarily to achieve high accuracy, but did not necessarily consider throughput as a metric of importance.

Throughput-utilization. Figure 1b plots each CNN according to its achieved throughput and GPU utilization. This plot looks similar to that in Figure 1a, but with CNNs having a more diverse range of GPU utilizations, plotted on the y-axis. We make two primary observations from this figure:

(1) The CNNs surveyed here tend not to have both high throughput and high GPU utilization. Rather, the CNNs that achieve higher throughput tend to have lower GPU utilization. This is likely due to these CNNs performing fewer FLOPs than larger CNNs, which can increase throughput, but often at the expense of GPU utilization.

(2) Sampled CNNs that are on the lower end of the spectrum in terms of throughput have a wide variety of GPU utilizations. There are many CNNs that achieve throughput of less than 10000 samples per second. Among these, we see CNNs that vary in GPU utilization from near 0% to near 90%. Given that the CNNs in this range have similar throughput, the primary factor leading to their varying GPU utilizations must be their FLOP count. This indicates either that (a) those CNNs within this band that achieve higher GPU utilization leverage operations that are more efficient on the GPU, or (b) those CNNs within this band that achieve lower GPU utilization leverage operations that are less efficient on the GPU. It is likely a case that we see a mix of these two options for different sampled CNNs.

GPU utilization-accuracy. Figure 1c plots each CNN according to its achieved GPU utilization and accuracy. We generally see a positive correlation between GPU utilization and accuracy. We investigate and exploit this correlation further in §4.

3.3 Opportunities to increase GPU utilization

Recall the prerequisite outlined in §2.1 for achieving high GPU utilization: arithmetic intensity must be greater than the compute-to-memory-bandwidth ratio (CMR) of the GPU on which a CNN runs. We next analyze the arithmetic intensities of the CNNs surveyed above to determine opportunities to improve GPU utilization.

Figure 2a plots the Pareto frontier between throughput and accuracy (i.e., Figure 1b) but with each CNN marked by whether its FP16 arithmetic intensity is greater or less than the FP16 CMR of the V100 GPU (139). As expected, we find that those CNNs that are on the higher end of the spectrum in terms of GPU utilization typically have arithmetic intensity greater than the CMR of the V100, while those with lower GPU utilization typically have arithmetic intensity below the CMR of the V100.

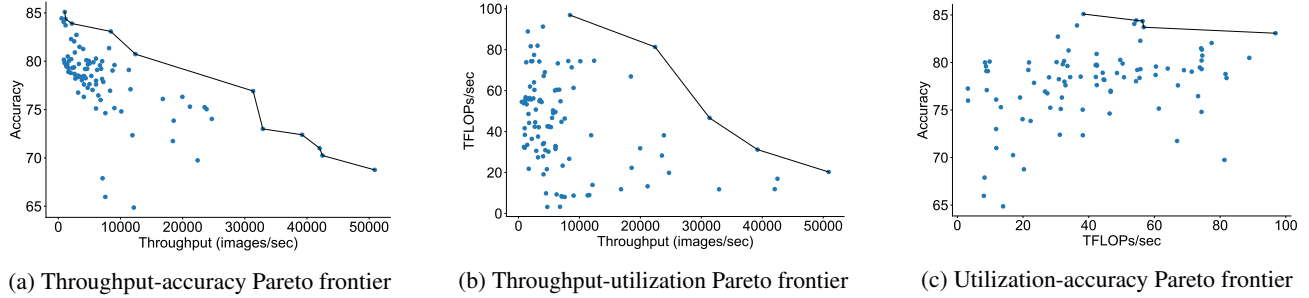


Figure 1. Pareto frontiers between metrics of accuracy, throughput, and GPU utilization. CNNs on the Pareto frontier are connected by a solid black line.

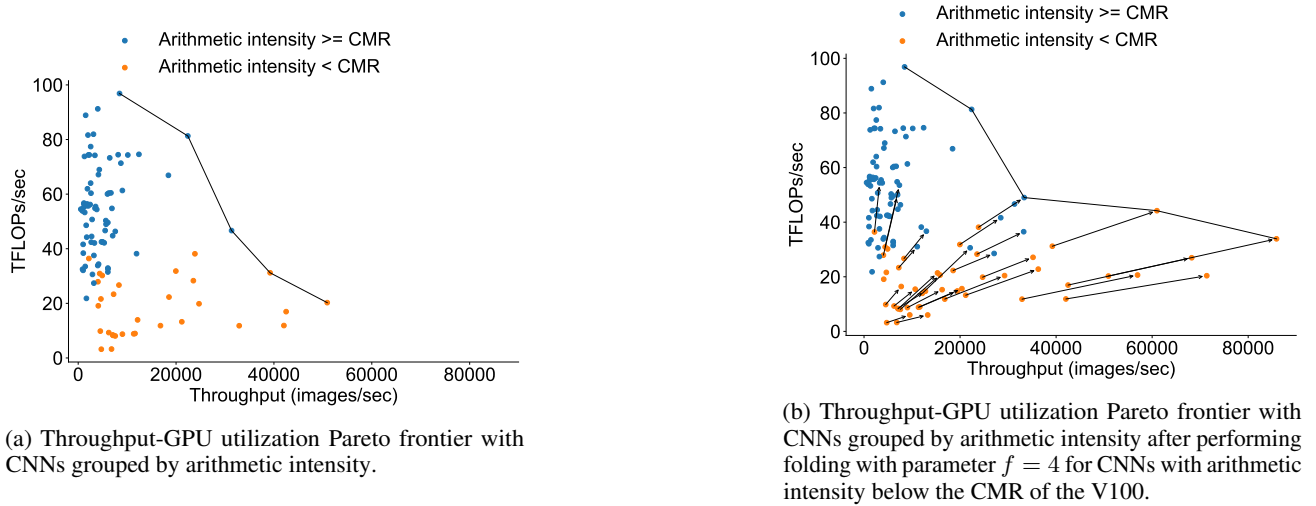


Figure 2. Pareto frontiers between throughput and GPU utilization when grouping CNNs based on whether their FP16 arithmetic intensity is greater or less than the the FP16 CMR of the V100 GPU (139). Figure (b) shows the same plot with the changes in throughput and GPU utilization made possible for performing a folding transformation with $f = 4$ on those CNNs with low arithmetic intensity.

The many CNNs with arithmetic intensity lower than the CMR of the V100 offer opportunities for potentially improving both throughput and GPU utilization by increasing arithmetic intensity. We next evaluate how a recently-proposed technique, FoldedCNNs (Kosaian et al., 2021), could potentially be used to transform these CNNs to increase arithmetic intensity. FoldedCNNs involve restructuring the inputs to a CNN as well as small changes to the CNN itself. Under a FoldedCNN, rather than operating over a batch of N images each with C channels (e.g., $C = 3$ for RGB images), a FoldedCNN instead operates over a batch of $\frac{N}{f}$ inputs, each with Cf channels, consisting of f images stacked along the channels dimension. The FoldedCNN then infers over these “combined” images. In addition to this restructuring of inputs, a FoldedCNN also increases the width of each layer of the CNN by a factor of \sqrt{f} (e.g., increasing the number of input and output channels of a convolutional layer by a factor of \sqrt{f}). This overall transformation performed by FoldedCNNs is referred to as “folding.” Under certain settings, this transformation is proven to transform a CNN

such that it performs nearly the same number of FLOPs, but with a reduction in memory traffic by a factor of \sqrt{f} . This leads to FoldedCNNs increasing arithmetic intensity under these settings by a factor of \sqrt{f} .

These modifications made by a FoldedCNN require the CNN to be retrained, and the new structure of inputs of a FoldedCNN appears to make the task of a FoldedCNN more challenging, which often leads to lower accuracy. For the purposes of our discussion here, we will focus only on the potential of FoldedCNNs to improve the GPU utilization of CNNs surveyed above, leaving accuracy considerations separate.

Figure 2b shows the throughput and GPU utilization achieved by each CNN when those CNNs with arithmetic intensity below the CMR of the V100 have been folded using parameter $f = 4$. For each CNN that has been modified, we connect an arrow starting from the CNN’s original throughput and GPU utilization to the new throughput and GPU utilization achieved after folding. We make the following

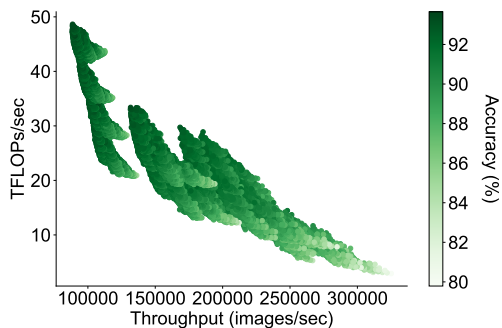


Figure 3. Throughput, GPU utilization, and accuracy of each CNN from the NATS-Bench size search space. Note that each CNN achieves less than 60% of the peak FLOPs/sec. of the V100 GPU.

observations:

1. *Techniques to increase arithmetic intensity expand the Pareto frontier between throughput and GPU utilization.* Figure 2b shows that the application of folding significantly increases the throughput and GPU utilization of CNNs on the Pareto frontier. For example, one CNN on the Pareto frontier increases in both throughput and GPU utilization by a factor of roughly 1.5.
2. *Further room for improving GPU utilization by increasing arithmetic intensity remains.* While many of the CNNs transformed in Figure 2b significantly increase in throughput and GPU utilization, many of the transformed CNNs still have arithmetic intensity lower than the CMR of the V100 (i.e., the dots at the beginning and end of the arrow have the same color). This indicates that further improvements in arithmetic intensity may lead to further increases in throughput and GPU utilization, if done judiciously. One technique to do so could be to increase the parameter f in folding, as the theoretical increase in arithmetic intensity resulting from folding scales with \sqrt{f} . However, doing so is likely to cause significant accuracy degradation; in the original FoldedCNNs evaluation, accuracy began to noticeably degrade at $f = 4$ (Kosaian et al., 2021). If this challenge of maintaining high accuracy could be circumvented, further increasing arithmetic intensity via folding would be a natural solution.

4 ACCELERATING NAS BY USING GPU UTILIZATION?

We now switch gears to analyzing another finding from §3: the positive correlation between accuracy and GPU utilization observed in Figure 1c. Specifically, we explore the opportunity to potentially use this correlation to leverage GPU utilization as a lightweight replacement metric for accuracy in traditional NAS search.

4.1 Positive correlation between accuracy and GPU utilization

Figure 1c illustrated a positive correlation between the GPU utilization of a CNN and the accuracy achieved by the CNN.

To further analyze this correlation in the context of NAS, we analyze CNNs from the NATS-Bench (Dong et al., 2021) “size search space.” NATS-Bench is a NAS benchmarking suite that contains the accuracies and model statistics (e.g., parameter count) for a large number of CNN architectures sampled from a pre-specified search space. This allows researchers to experiment with changes in the NAS search algorithm itself quickly without the need to train each candidate architecture.

We specifically focus on the NATS-Bench “size search space.” Each CNN within this search space has the same depth (in terms of number of convolutional layers) and the same layer types (e.g., filter spatial resolution). However, each architecture differs in the number of channels per layer. We leverage the accuracy measurements reported within NATS-Bench for the CIFAR-10 dataset. We measure throughput and GPU utilization using the same evaluation setup described in §3.1.

Figure 3 plots the throughput, GPU utilization, and accuracy of each CNN from the NATS-Bench size search space. While there are a number of trends of interest in this plot, we focus on one finding: *as GPU utilization increases, accuracy typically increases.* This is illustrated in Figure 3 by noting that the shade of each point in the plot typically gets darker with increasing GPU utilization. This observation is likely explained by an increase in FLOP count for CNNs with higher GPU utilization, as increasing FLOP count is likely to increase both accuracy and GPU utilization. Furthermore, within the vertical bands of CNNs with near equal throughput in Figure 3, we typically observe an increase in accuracy with increasing GPU utilization.

Takeaway. Both across general-purpose CNNs (§3) as well as a benchmark NAS search space, we find a positive correlation between GPU utilization and accuracy. In the remaining portions of this section, we investigate how this correlation can potentially be exploited to reduce the number of samples in NAS that require accuracy evaluation.

4.2 Background on sample-based NAS

We first provide background on the sample-based NAS procedure that we aim to accelerate and the target Pareto frontier that we aim to optimize for.

4.2.1 Sample-based NAS objective and procedure

We consider NAS to be parameterized by a search space \mathcal{S} consisting of neural network architectures to be considered,

along with a set of evaluation functions \mathcal{F} that are used to score candidate architectures from the search space. The goal of NAS is to find the set of neural networks from \mathcal{S} that lie on the Pareto frontier of \mathcal{F} . Concretely, the Pareto frontier contains all neural networks which are not dominated by another neural network in all evaluation functions in \mathcal{F} .

We now describe the search procedure used in sample-based NAS. For a comprehensive survey of other NAS methods, please see [Elsken et al. \(2019\)](#). To find the desired Pareto frontier, sample-based NAS iteratively selects a neural network s from \mathcal{S} , evaluates s on each evaluation function in \mathcal{F} , adds s to its running Pareto frontier, and (optionally) updates its selection criteria based on the evaluation of s . There are many methods that can be used to select neural networks from the search space, such as random search ([Li & Talwalkar, 2020](#)), evolutionary search ([Real et al., 2019](#)), and reinforcement learning ([Zoph & Le, 2016](#)). In this work, we abstract away the exact technique being used to guide the search process, as our focus is on the evaluation functions themselves.

Associated with each evaluation function $f_i \in \mathcal{F}$ is a time that it takes to perform the evaluation t_i .¹ The time that it takes to perform an iteration of the above search procedure is determined by either the sum of all such evaluation times (if evaluation functions are executed serially), or the maximum evaluation time (if evaluation functions are executed in parallel). To bound the overall time that NAS can run, NAS is typically parameterized with a “time budget” T_B after which the search is terminated. Thus, the Pareto frontier returned by NAS may not be the true Pareto frontier of the entire search space \mathcal{S} in cases where NAS is unable to exhaustively enumerate through the search space within the prescribed time budget.

4.2.2 Accuracy, application-level throughput frontier

In this work, we focus on one concrete instantiation of the sample-based NAS procedure described in §4.2.1: that when the target Pareto frontier is of accuracy and application-level throughput. In this scenario, \mathcal{F} consists of two evaluation functions: one that evaluates the accuracy of a given neural network (denoted f_A), and one that evaluates the inference-time application-level throughput of the neural network in inputs/sec (denoted f_T). A NAS search procedure may define an objective ranking function for a given neural network based on a combination of these two evaluation functions.

¹Here, we make a simplifying assumption that each evaluation function takes a constant amount of time, regardless of the neural network over which it operates. This will not be the case in practice, as evaluation functions such as accuracy will take variable amounts of time, depending on the neural network being evaluated. For the purposes of the present discussion, which will be about comparing evaluation function times across evaluation functions, such a simplifying assumption suffices.

Algorithm 1 Sample-based NAS for finding the accuracy-application-level throughput Pareto frontier

```

t ← 0
while t < TB do
  s ← sample( $\mathcal{S}$ )
  eA ← fA(s)
  eT ← fT(s)
  rs ← r(eA, eT)
  t ← t + max(tA, tT) {Assumes fA and fT run in parallel}
  if onFrontier(eA, eT) then
    addToFrontier(s, eA, eT) {Removes points from running frontier, if necessary}
  end if
  {Optionally update sampling function based on rs (e.g., if using reinforcement-learning-based search)}
end while

```

For example, a ranking function r derived from that used by [Tan et al. \(2019\)](#) combining these evaluation functions might be:

$$r(s) = \frac{f_A(s)}{100} \times \left[\frac{f_T(s)}{G_T} \right]^w \quad (3)$$

where G_T is a constant, target application-level throughput, and w controls how much weight to give application-level throughput in ranking. Algorithm 1 illustrates this overall search procedure.

Dominant cost of sample-based NAS. Ideally, sample-based NAS would be able to sample all possible neural networks from the search space. However, this is precluded by the cost of evaluation functions, the large sizes of search spaces used in practice, and limitations on the compute resources that can be devoted to NAS.

In particular, the primary bottleneck that contributes to the large time and resource cost of sample-based NAS is *accuracy evaluation* (i.e., f_A). Evaluating the accuracy of a sample requires training the sampled neural network, which can take on the order of GPU-days, if done to convergence. In contrast, evaluating inference-time application-level throughput (i.e., f_T) is much less expensive, taking at most minutes on a GPU.

Reducing costs. Based on the dominance of evaluating accuracy on the overall time and resource cost of sample-based NAS, it is clear that the time and resource cost of sample-based NAS could be greatly reduced by either (or both of): (1) reducing the time and resources required for accuracy evaluation (i.e., reducing t_A), (2) reducing the number of samples that require accuracy evaluation. These two opportunities toward speeding up sample-based NAS complement one another.

A number of works have developed techniques toward op-

portunity (1) of reducing the time and resource costs of accuracy evaluation. The key approach used therein is to approximate accuracy evaluation. Examples of such techniques include training on a cheaper, proxy dataset (e.g., CIFAR-10 instead of ImageNet) (e.g., (Liu et al., 2018)); training with a smaller neural network than the true neural network sampled from the search space; training on smaller inputs than those used in the true task (e.g., reducing image resolution); stopping training earlier than reaching final convergence (e.g., (Li & Talwalkar, 2020)); and sharing weights between distinct sampled neural networks (e.g., (Pham et al., 2018)). These techniques have some potential downsides, such as the requirement for the availability of a representative proxy dataset (which may not be available in all domains), and assumptions about the fidelity of the accuracy approximation being made. However, as a whole, these techniques remain promising for speeding up sample-based NAS.

Toward opportunity (2), reducing the number of neural networks for which accuracy evaluation is required, the primary techniques used involve improving the sampling algorithm itself. This may entail using some form of learning in the sampling procedure in attempt to determine which samples are likely to achieve high performance along the Pareto frontier, based on samples that one has already evaluated.

In this section, we explore an alternative path toward opportunity (2) that does not require expensive learning procedures. We next describe this approach.

4.3 Opportunity: leveraging approximate filtering

We explore the use of *approximate filtering* to accelerate sample-based NAS. In this subsection, we provide background on approximate filtering, how it could be applied within sample-based NAS, and the potential reduction in NAS time and resource cost it could introduce.

4.3.1 Approximate filtering

Approximate filtering is a common technique leveraged in data systems and neural network inference systems to alleviate the need to evaluate an expensive predicate on all samples. The key method used in approximate filtering is to introduce an inexpensive predicate that approximates the true, expensive predicate. Due to the inexpensive nature of this approximate predicate, the approximate predicate can be evaluated on many more samples than the expensive one. Approximate filtering then works by evaluating the inexpensive approximate predicate on all samples to filter out those that one is confident will not satisfy the expensive predicate, and applying the true, expensive predicate on only those samples that satisfy the inexpensive predicate. Thus, approximate filtering accelerates search by reducing the number of samples on which the expensive predicate

must be applied. This approach has been widely used in analytics systems through techniques such as model specialization (Kang et al., 2017).

4.3.2 Applying approximate filtering to NAS

Our aim is to apply approximate filtering to reduce the number of neural networks that must undergo full accuracy evaluation (i.e., f_A) in sample-based NAS. To do so, we introduce an approximate evaluation function f_P that has an evaluation time $t_P \ll t_A$. With such an approximate evaluation function in place, the approximate-filtering-augmented NAS procedure is as follows: (1) find the Pareto frontier (\mathcal{P}_P) parameterized by application-level throughput and this approximate evaluation function by evaluating every neural network (or most) from the search space in terms of application-level throughput and the approximate function; (2) evaluate accuracy on each neural network in \mathcal{P}_P to obtain an approximate accuracy-application-level throughput Pareto frontier $\widehat{\mathcal{P}}_A$.

4.4 Utilization-based approximate filtering

An approach to approximate filtering for sample-based NAS requires the use of an approximate evaluation function that (1) correlates closely with accuracy (so as to preserve the quality of the final Pareto frontier found), (2) is far less expensive to evaluate than accuracy, and (3) significantly reduces the number of samples that require full accuracy evaluation.

Based on our analysis of the NATS-Bench search space in §4.1, we question whether GPU utilization could be a suitable approximate evaluation metric. Indeed, GPU utilization satisfies the first two criteria listed above: (1) As shown in §4.1, GPU utilization correlates to accuracy for this search space; (2) GPU utilization is significantly less expensive to measure than accuracy, as it involves multiplying throughput by FLOP count.

To analyze the third criterion, we count the number of networks in the Pareto frontier between throughput and GPU utilization, compared to the size of the total search space. We find that this Pareto frontier contains 144 networks, whereas the NATS-Bench size search space contains 32767 networks as a whole. This illustrates that leveraging GPU utilization as an approximate evaluation function could significantly reduce the number of networks that require full accuracy evaluation, as only those within this Pareto frontier would need to be evaluated.

Why not use FLOP count? A natural question that may arise is whether an alternative approximate evaluation function besides GPU utilization may suffice, such as using the FLOP count of the CNN. After all, FLOP count typically does correlate with the accuracy of a CNN. However, we

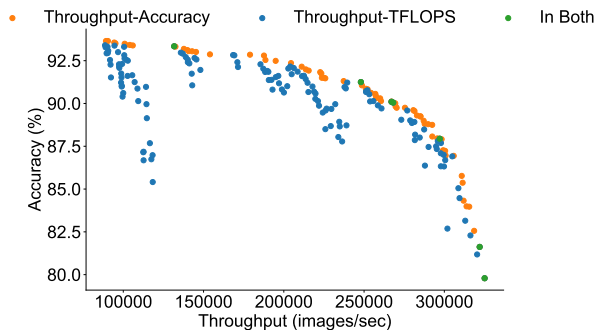


Figure 4. CNNs plotted in terms of their accuracy and throughput. Orange networks are those on the true throughput-accuracy Pareto frontier, blue networks are those on the throughput-utilization frontier, and green networks are those in both frontiers.

find that using FLOP count as an approximate evaluation function leads to an approximate Pareto frontier for the NATS-Bench size search space with 255 evaluation points, which is significantly more than the 144 when using GPU utilization. Therefore, we opt for using GPU utilization as an approximate evaluation function in this work.

How close to the true Pareto frontier is the approximate Pareto frontier? Recall that the first step in leveraging approximate filtering for NAS is to generate an approximate Pareto frontier from which we will sample networks to evaluate accuracy. In order for the final results of this approximate search to maintain high fidelity to the original search, it is important that this approximate Pareto frontier contain many points close to those on the desired Pareto frontier. Figure 4 compares the final throughput and accuracy of CNNs on this approximate frontier to those on the true throughput-accuracy frontier. We observe that the approximate frontier contains many networks that are very close to those on the true frontier, but also contains a number of spurious networks that are far from the true frontier. These spurious points will be eliminated by the second step, which performs accuracy evaluation on this approximate frontier, leading to an overall Pareto frontier close to the true frontier. Thus, we conclude that the overall approximate search procedure proposed will obtain a Pareto frontier close to that desired.

4.5 Evaluating utilization-based approximate filtering

We now evaluate whether this approach of approximate filtering can reach better final Pareto frontiers than performing traditional NAS under the same time budget.

In doing so, we adopt the search simulation infrastructure developed in NATS-Bench. We compare our proposed approach to using sampling-based NAS in which the sampling

function is learned via REINFORCE with the reward function given by Equation 3 with $G_T = 175000$ and $w = 0.07$, borrowing this from Tan et al. (2019). We run each approach for 110000 timestep in the NATS-Bench search simulation procedure: this is sufficient time for the approximate search technique to both evaluate the approximate metric on all points in the search space and to perform accuracy evaluation on the approximate Pareto frontier.

Figure 5 shows the Pareto frontier returned by the approximate filtering search procedure compared to the true accuracy-throughput Pareto frontier for this search space. The Pareto frontier returned by approximate search is similar to the true Pareto frontier: while the approximate Pareto frontier does contain fewer points than the true Pareto frontier, those points which are returned lie close to the true Pareto frontier. The small differences in accuracy and throughput between points on the approximate frontier and those on the true frontier may be indiscernible for many applications.

Figure 6 plots the Pareto frontiers returned by using reinforcement learning in NAS as described above, compared to the true Pareto frontier. We show this for nine different random seeds, as this technique is only able to sample a subset of the networks from the search space, and thus depends on the initial network one starts with. We generally find that the Pareto frontiers returned via this reinforcement-learning-based approach are also close to the true Pareto frontier. Some seeds show exceptions: for example, in seed 7000, the returned Pareto frontier is noticeably worse than the true Pareto frontier.

The results between reinforcement-learning-based search and leveraging the approximate filtering technique proposed above are mostly similar. This indicates that, while leveraging approximate filtering may be promising, it does not yield significant improvements in the returned Pareto frontier, at least for the NATS-Bench size search space.

While the evaluation results above have not yielded significant benefits in terms of NAS search time or the quality of the networks returned from search, leveraging GPU utilization for approximate filtering within NAS may still raise benefits not revealed above. In particular, in many setups, evaluating accuracy may require a distributed training setup. This setup not only occupies significant cluster compute resources (e.g., GPUs), but also consumes considerable network traffic for distributed training and storage system bandwidth for data loading (Mohan et al., 2021). In contrast, evaluating GPU utilization requires a single GPU, and does not consume any network or storage bandwidth. This reduces contention for these often-shared resources in datacenter and cloud settings. Thus, leveraging approximate filtering in NAS could make NAS more resource efficient.

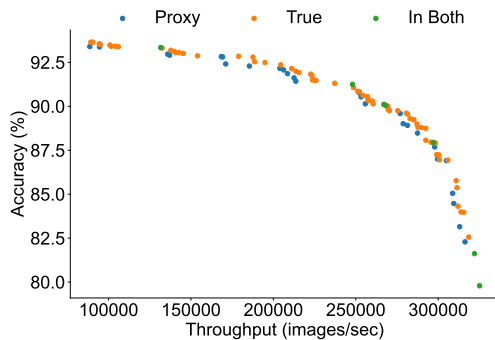


Figure 5. Accuracy-throughput Pareto frontier found by leveraging GPU utilization as an approximate evaluation function, via the algorithm described in §4.3.2. “Proxy” refers to points returned by this approximate search. “True” refers to points returned by the traditional throughput-accuracy search. “In Both” refers to points that lie in each set of returned values.

5 CONCLUSION

This work has explored the GPU utilization of high-throughput CNN inference as well as opportunities to leverage GPU utilization to improve NAS. We have evaluated the GPU utilization of popular CNNs, showing that these CNNs exhibit a wide range of GPU utilization. Many of these CNNs exhibit promising potential for improving GPU utilization, opening opportunities for future work to design CNNs that better utilize GPUs or system-level techniques to increase GPU utilization. Based on correlations between GPU utilization and accuracy, we next investigated the potential of using GPU utilization as a lightweight approximate evaluation metric in place of accuracy in NAS. We adapt the well-studied technique of approximate filtering from data systems literature to NAS. While the results from this preliminary study did not yield significant improvements in NAS search time or quality, we believe that future NAS techniques could benefit from considering leveraging GPU utilization in place of accuracy during NAS.

Through this exploration, this paper illustrates that GPU utilization is an important metric to consider both in terms of improving operational efficiency and CNN throughput, as well as for potentially improving NAS algorithms.

REFERENCES

Cai, H., Gan, C., Wang, T., Zhang, Z., and Han, S. Once-for-All: Train One Network and Specialize it for Efficient Deployment. In *International Conference on Learning Representations (ICLR 19)*, 2019.

Chen, T., Moreau, T., Jiang, Z., Zheng, L., Yan, E., Shen, H., Cowan, M., Wang, L., Hu, Y., Ceze, L., Guestrin, C., and Krishnamurthy, A. TVM: An automated end-

to-end optimizing compiler for deep learning. In *13th USENIX Symposium on Operating Systems Design and Implementation (OSDI 18)*, 2018.

Dong, X., Liu, L., Musial, K., and Gabrys, B. NATS-Bench: Benchmarking NAS Algorithms for Architecture Topology and Size. *IEEE Transactions on Pattern Analysis and Machine Intelligence (IEEE TPAMI)*, 2021.

Elsken, T., Metzen, J. H., and Hutter, F. Neural Architecture Search: A Survey. *Journal of Machine Learning Research (JMLR)*, 20(55):1–21, 2019.

Gu, J., Chowdhury, M., Shin, K. G., Zhu, Y., Jeon, M., Qian, J., Liu, H., and Guo, C. Tiresias: A GPU Cluster Manager for Distributed Deep Learning. In *16th USENIX Symposium on Networked Systems Design and Implementation (NSDI 19)*, 2019.

Jain, P., Mo, X., Jain, A., Subbaraj, H., Durrani, R. S., Tumanov, A., Gonzalez, J., and Stoica, I. Dynamic Space-Time Scheduling for GPU Inference. In *NeurIPS Workshop on Systems for Machine Learning*, 2018.

Jia, Z., Maggioni, M., Staiger, B., and Scarpazza, D. P. Dissecting the NVIDIA Volta GPU Architecture via Microbenchmarking. *arXiv preprint arXiv:1804.06826*, 2018.

Kang, D., Emmons, J., Abuzaid, F., Bailis, P., and Zaharia, M. NoScope: Optimizing Neural Network Queries over Video at Scale. *Proceedings of the VLDB Endowment*, 10(11):1586–1597, 2017.

Kosaian, J., Phanishayee, A., Philipose, M., Dey, D., and Rashmi, K. V. Boosting the Throughput and Accelerator Utilization of Specialized CNN Inference Beyond Increasing Batch Size. In *Proceedings of the 38th International Conference on Machine Learning (ICML 21)*, 2021.

Li, L. and Talwalkar, A. Random Search and Reproducibility for Neural Architecture Search. In *Uncertainty in Artificial Intelligence (UAI 20)*, 2020.

Liu, H., Simonyan, K., and Yang, Y. DARTS: Differentiable Architecture Search. In *International Conference on Learning Representations (ICLR 18)*, 2018.

Mohan, J., Phanishayee, A., Raniwala, A., and Chidambaram, V. Analyzing and Mitigating Data Stalls in DNN Training. *Proceedings of the VLDB Endowment*, 14(5):771–784, 2021.

Molchanov, P., Hall, J., Yin, H., Kautz, J., Fusi, N., and Vahdat, A. HANT: Hardware-Aware Network Transformation. *arXiv preprint arXiv:2107.10624*, 2021.

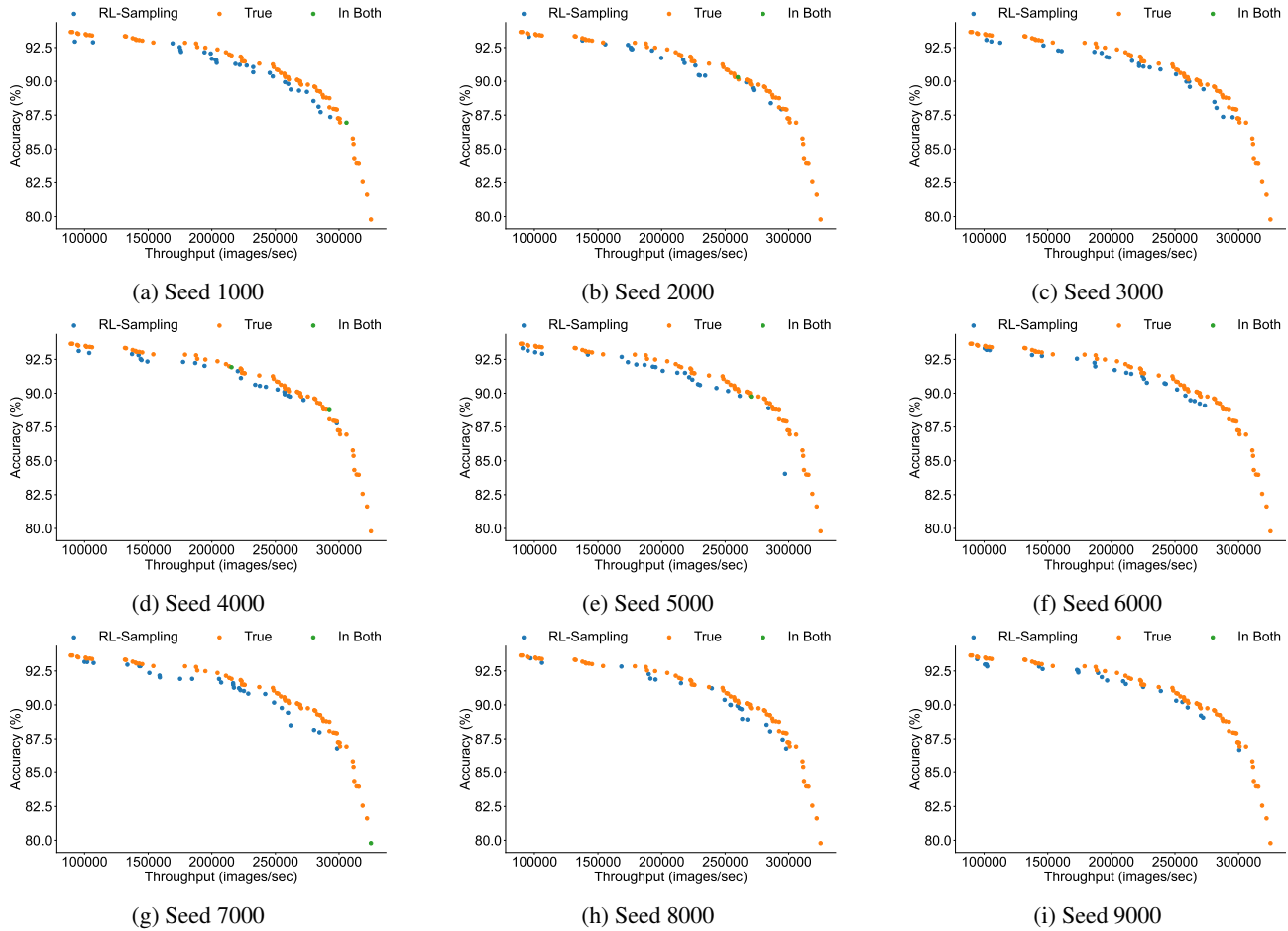


Figure 6. Accuracy-throughput Pareto frontier achieved by reinforcement-learning-based NAS (blue) with nine different beginning random seeds, compared to the true Pareto frontier over the NATS-Bench size search space (orange). “In Both” refers to points that lie in each set of returned values.

Narayanan, D., Santhanam, K., Phanishayee, A., and Zaharia, M. Accelerating Deep Learning Workloads Through Efficient Multi-Model Execution. In *NeurIPS Workshop on Systems for Machine Learning*, 2018.

NVIDIA. NVIDIA A100 GPU. <https://www.nvidia.com/en-us/data-center/a100/>, a. Last accessed 23 November 2021.

NVIDIA. NVIDIA Tensor Cores <https://www.nvidia.com/en-us/data-center/tensor-cores/>, b. Last accessed 23 August 2021.

NVIDIA. NVIDIA TensorRT. <https://developer.nvidia.com/tensorrt>, c. Last accessed 23 August 2021.

NVIDIA. NVIDIA Tesla V100 GPU Architecture. Technical Report WP-08608-001_v1.1, 2017.

NVIDIA. NVIDIA Turing GPU Architecture. Technical Report WP-09183-001_v01, 2018.

Pham, H., Guan, M., Zoph, B., Le, Q., and Dean, J. Efficient Neural Architecture Search via Parameters Sharing. In *Proceedings of the 35th International Conference on Machine Learning (ICML 18)*, 2018.

Real, E., Aggarwal, A., Huang, Y., and Le, Q. V. Regularized Evolution for Image Classifier Architecture Search. In *Proceedings of the AAAI Conference on Artificial Intelligence (AAAI 19)*, 2019.

Redmon, J., Divvala, S., Girshick, R., and Farhadi, A. You Only Look Once: Unified, Real-Time Object Detection. In *Proceedings of the IEEE Conference on Computer Vision and Pattern Recognition (CVPR 16)*, 2016.

Ridnik, T., Lawen, H., Noy, A., Ben Baruch, E., Sharir, G., and Friedman, I. Tresnet: High Performance GPU-Dedicated Architecture. In *Proceedings of the IEEE/CVF Winter Conference on Applications of Computer Vision (WACV 21)*, 2021.

- Russakovsky, O., Deng, J., Su, H., Krause, J., Satheesh, S., Ma, S., Huang, Z., Karpathy, A., Khosla, A., Bernstein, M., Berg, A. C., and Fei-Fei, L. ImageNet Large Scale Visual Recognition Challenge. *International Journal of Computer Vision (IJCV)*, 115(3):211–252, 2015. doi: 10.1007/s11263-015-0816-y.
- Tan, M. and Le, Q. EfficientNet: Rethinking Model Scaling for Convolutional Neural Networks. In *Proceedings of the 36th International Conference on Machine Learning (ICML 19)*, 2019.
- Tan, M., Chen, B., Pang, R., Vasudevan, V., Sandler, M., Howard, A., and Le, Q. V. MnasNet: Platform-Aware Neural Architecture Search for Mobile. In *Proceedings of the IEEE/CVF Conference on Computer Vision and Pattern Recognition (CVPR 19)*, 2019.
- Wang, S., Yang, P., Zheng, Y., Li, X., and Pekhimenko, G. Horizontally Fused Training Array: An Effective Hardware Utilization Squeezer for Training Novel Deep Learning Models. *The Fourth Conference on Machine Learning and Systems (MLSys 21)*, 2021.
- Wightman, R. Pytorch image models. <https://github.com/rwightman/pytorch-image-models>, 2019.
- Williams, S., Waterman, A., and Patterson, D. Roofline: an Insightful Visual Performance Model for Multicore Architectures. *Communications of the ACM*, 52(4):65–76, 2009.
- Wu, B., Dai, X., Zhang, P., Wang, Y., Sun, F., Wu, Y., Tian, Y., Vajda, P., Jia, Y., and Keutzer, K. FBNet: Hardware-Aware Efficient ConvNet Design via Differentiable Neural Architecture Search. In *Proceedings of the IEEE/CVF Conference on Computer Vision and Pattern Recognition*, pp. 10734–10742, 2019.
- Xiao, W., Bhardwaj, R., Ramjee, R., Sivathanu, M., Kwatra, N., Han, Z., Patel, P., Peng, X., Zhao, H., Zhang, Q., et al. Gandiva: Introspective Cluster Scheduling for Deep Learning. In *13th USENIX Symposium on Operating Systems Design and Implementation (OSDI 18)*, 2018.
- Yu, P. and Chowdhury, M. Salus: Fine-Grained GPU Sharing Primitives for Deep Learning Applications. In *The Third Conference on Machine Learning and Systems (MLSys 20)*, 2020.
- Zhou, Y., Ebrahimi, S., Arık, S. Ö., Yu, H., Liu, H., and Diamos, G. Resource-Efficient Neural Architect. *arXiv preprint arXiv:1806.07912*, 2018.
- Zoph, B. and Le, Q. V. Neural Architecture Search with Reinforcement Learning. *arXiv preprint arXiv:1611.01578*, 2016.

A RESULTS FROM SURVEYED CNNs

Tables 1 and 2 show the results from the survey of CNNs performed in §3. We additionally depict with “X” whether a CNN is on a particular Pareto frontier.

Table 1. Models evaluated in survey. Accuracy is in percentage and throughput is in images/sec.

Name	Accuracy	Throughput	TFLOPs/sec	On Tput.-Acc. Frontier?	On TFLOPS-Acc. Frontier?	On Tput.-TFLOPS Frontier?
tresnet_m	83.08	8444.73	96.86	X	X	X
efficientnetv2_m	85.10	1039.29	38.39	X	X	-
seresnet152d	84.36	1175.21	56.39	X	X	-
gernet_s	76.92	31344.26	46.65	X	-	X
regnetx_004	72.40	39215.73	31.19	X	-	X
regnetx_002	68.76	50893.82	20.26	X	-	X
efficientnetv2_s	83.90	2176.89	36.42	X	-	-
gernet_m	80.73	12411.49	74.58	X	-	-
ofanet-v100_@6ms	73.00	32903.61	11.80	X	-	-
ofanet-v100_@5ms	71.00	42038.86	11.87	X	-	-
regnety_002	70.25	42492.74	16.96	X	-	-
resnetrs270	84.43	535.07	54.49	-	X	-
resnetrs152	83.71	1169.59	56.72	-	X	-
resnet18	69.75	22409.05	81.30	-	-	X
resnetrs200	84.07	858.29	53.86	-	-	-
regnety_032	82.72	2915.10	30.60	-	-	-
resnetrs101	82.29	2062.88	55.70	-	-	-
tresnet_xl	82.05	2552.27	77.41	-	-	-
tresnet_l	81.49	3411.52	74.21	-	-	-
wide_resnet50	81.46	4002.17	91.23	-	-	-
gernet_l	81.35	8166.70	74.43	-	-	-
seresnext50_32x4d	81.27	3998.37	33.85	-	-	-
seresnext101_32x4d	80.90	2657.49	42.39	-	-	-
repvgg_b3	80.49	1526.05	88.88	-	-	-
seresnet50	80.27	6059.46	49.59	-	-	-
repvgg_b3g4	80.21	2082.79	74.35	-	-	-
dpn107	80.16	887.80	32.49	-	-	-
efficientnet_b2	80.10	4518.30	9.83	-	-	-
cpresnext50	80.04	4911.09	30.20	-	-	-
dpn92	80.01	1677.89	21.82	-	-	-
ofanet-flops@595M	80.00	7063.24	8.41	-	-	-
resnetrs50	79.89	5189.78	44.55	-	-	-
dpn131	79.82	1002.03	32.09	-	-	-
resnext50_32x4d	79.77	5011.84	42.41	-	-	-
regnety_064	79.72	3313.35	42.11	-	-	-
resnext50d_32x4d	79.68	4755.81	42.52	-	-	-
dpn98	79.64	1435.61	33.51	-	-	-
ofanet-flops@482M	79.60	9035.14	8.72	-	-	-
cpresnet50	79.57	6691.55	60.45	-	-	-
hrnet_w64	79.47	1277.18	73.81	-	-	-
repvgg_b2g4	79.37	2542.93	64.03	-	-	-
resnext101_32x8d	79.31	2265.54	74.37	-	-	-
hrnet_w48	79.30	1612.77	55.73	-	-	-
regnety_040	79.22	6893.49	54.78	-	-	-
dpn68b	79.22	4644.92	21.61	-	-	-
regnetx_080	79.19	4313.02	68.97	-	-	-
ofanet-flops@389M	79.10	11343.95	8.84	-	-	-
efficientnet_b1	79.10	6249.63	9.29	-	-	-

Table 2. (Continued) Models evaluated in survey. Accuracy is in percentage and throughput is in images/sec.

Name	Accuracy	Throughput	TFLOPs/sec	On Tput.-Acc. Frontier?	On TFLOPS-Acc. Frontier?	On Tput.-TFLOPS Frontier?
resnet50	79.04	8722.50	71.34	-	-	-
hrnet_w40	78.92	1742.82	44.24	-	-	-
hrnet_w44	78.90	1632.27	48.59	-	-	-
repvgg_b2	78.79	1999.03	81.63	-	-	-
dla169	78.69	2610.92	60.35	-	-	-
dla102x	78.51	3209.39	37.54	-	-	-
regnetx_040	78.48	5317.33	42.16	-	-	-
dla60_res2net	78.46	4167.03	34.36	-	-	-
hrnet_w32	78.45	2842.49	50.72	-	-	-
dla60_res2next	78.44	4035.40	27.91	-	-	-
seresnet101	78.38	3552.61	55.46	-	-	-
repvgg_b1	78.37	3120.94	81.94	-	-	-
dla60x	78.25	4394.39	30.91	-	-	-
hrnet_w30	78.21	2745.27	44.51	-	-	-
regnetx_032	78.17	7045.64	44.76	-	-	-
dla102	78.03	3795.49	54.39	-	-	-
seresnext26t_32x4d	77.99	6081.96	32.60	-	-	-
regnety_016	77.86	7238.16	23.34	-	-	-
tv_resnext50_32x4d	77.62	5015.94	42.44	-	-	-
seresnext26d_32x4d	77.60	6070.07	32.92	-	-	-
repvgg_b1g4	77.59	4135.22	67.14	-	-	-
mixnet_m	77.26	4722.31	3.20	-	-	-
efficientnet_b0	77.10	11612.13	8.96	-	-	-
dla60	77.03	5507.80	46.66	-	-	-
regnetx_016	76.95	8326.46	26.69	-	-	-
hrnet_w18	76.76	3198.62	27.40	-	-	-
repvgg_a2	76.46	6444.23	73.28	-	-	-
dpn68	76.32	4105.41	19.10	-	-	-
regnety_008	76.32	19957.41	31.82	-	-	-
ofanet-v100_@11ms	76.10	16811.99	11.83	-	-	-
mixnet_s	75.99	6812.00	3.26	-	-	-
ofanet-v100_@9ms	75.30	21176.05	13.25	-	-	-
regnety_006	75.25	23534.66	28.30	-	-	-
repvgg_b0	75.15	9027.21	61.33	-	-	-
hrnet_w18_small_v2	75.11	6063.18	31.48	-	-	-
regnetx_008	75.04	23851.86	38.15	-	-	-
seresnet34	74.81	10143.47	74.33	-	-	-
dla34	74.63	7573.85	46.35	-	-	-
regnety_004	74.03	24692.65	19.85	-	-	-
regnetx_006	73.85	18555.66	22.30	-	-	-
hrnet_w18_small	72.34	11923.19	38.19	-	-	-
seresnet18	71.74	18435.65	66.89	-	-	-
dla60x_c	67.89	7120.45	8.28	-	-	-
dla46x_c	65.97	7567.59	8.06	-	-	-
dla46_c	64.87	12140.11	13.94	-	-	-